AJNR

Regional and Volumetric Parameters for Diffusion-Weighted WHO Grade II and III Glioma Genotyping: A Method Comparison

S.C. Thust, J.A. Maynard, M. Benenati, S.J. Wastling, L. Mancini, Z. Jaunmuktane, S. Brandner and H.R. Jäger

Regional and Volumetric Parameters for Diffusion-Weighted WHO Grade II and III Glioma Genotyping: A Method Comparison

S.C. Thust, J.A. Maynard, M. Benenati, S.J. Wastling, L. Mancini, Z. Jaunmuktane, S. Brandner, and H.R. Jäger

ABSTRACT

BACKGROUND AND PURPOSE: Studies consistently report lower ADC values in *isocitrate dehydrogenase* (*IDH*) wild-type gliomas than in *IDH* mutant tumors, but their methods and thresholds vary. This research aimed to compare volumetric and regional ADC measurement techniques for glioma genotyping, with a focus on *IDH* status prediction.

MATERIALS AND METHODS: Treatment-naïve World Health Organization grade II and III gliomas were analyzed by 3 neuroradiologist readers blinded to tissue results. ADC minimum and mean ROIs were defined in tumor and in normal-appearing white matter to calculate normalized values. T2-weighted tumor VOIs were registered to ADC maps with histogram parameters (mean, 2nd and 5th percentiles) extracted. Nonparametric testing (eta^2 and ANOVA) was performed to identify associations between ADC metrics and glioma genotypes. Logistic regression was used to probe the ability of VOI and ROI metrics to predict *IDH* status.

RESULTS: The study included 283 patients with 79 *IDH* wild-type and 204 *IDH* mutant gliomas. Across the study population, *IDH* status was most accurately predicted by ROI mean normalized ADC and VOI mean normalized ADC, with areas under the curve of 0.83 and 0.82, respectively. The results for ROI-based genotyping of nonenhancing and solid-patchy enhancing gliomas were comparable with volumetric parameters (area under the curve = 0.81–0.84). In rim-enhancing, centrally necrotic tumors (n = 23), only volumetric measurements were predictive (0.90).

CONCLUSIONS: Regional normalized mean ADC measurements are noninferior to volumetric segmentation for defining solid glioma *IDH* status. Partially necrotic, rim-enhancing tumors are unsuitable for ROI assessment and may benefit from volumetric ADC quantification.

ABBREVIATIONS: AUC = area under the curve; NAWM = normal-appearing white matter; min = minimum; 1p19q^{codel} = codeletion of the short arm of chromosome 1 and the long arm of chromosome 19; rADC = normalized ADC; WHO = World Health Organization

Diffuse gliomas of World Health Organization (WHO) grades II and III comprise a diverse group of tumors characterized by distinct genetic profiles and varied median survival.[1] Three major types of diffuse gliomas are found in adults: *isocitrate*

dehydrogenase (*IDH*) wild-type gliomas with a molecular profile of *IDH* wild-type glioblastoma, *IDH* mutant astrocytoma (with p53 and *ATRX chromatin remodeler* [*ATRX*] mutations), and the *IDH* mutant oligodendroglioma with a codeletion of the short arm of chromosome 1p and the long arm of chromosome 19q (*IDH* mutant/1p19q^{codel}).[2] In addition to these major intrinsic neoplasms, multiple other tumor types exist, for example, with alterations in the map kinase pathway (*B-Raf proto-oncogene, serine/threonine kinase* [*BRAF*] mutations), histone mutations, and the distinct group of ependymal tumors.

IDH wild-type astrocytomas share glioblastoma-specific genetic mutations such as combined chromosome 7 gain and

chromosome 10 loss, *epidermal growth factor receptor* (*EGFR*) amplification, and/or *telomerase reverse transcriptase* (*TERT*) promoter mutations[3] and have a short life expectancy.[3,4] Henceforth, with the term "*IDH* wild-type diffuse glioma," we will refer to molecular glioblastoma, *IDH* wild-type.

Rapid glioma genotyping is of prognostic importance and influences therapeutic planning; for example, *IDH* mutant/1p19q[codel] gliomas are responsive to chemotherapy,[5] whereas in 1p19q intact (*IDH* mutant/1p19q intact) tumors, maximum safe resection appears critical to improve outcomes.[6] It remains uncertain to what extent the strategy of maximal glioblastoma resection[7,8] could prolong survival for diffusely infiltrative *IDH* wild-type gliomas in the WHO grade II and III stages.

A number of imaging techniques have shown the potential for glioma genotype predictions. Of these, conventional MR imaging has the advantage of universal availability, but mostly provides visual-anatomic features, some of which have limited reproducibility.[9,10] Advanced MR imaging techniques such as perfusion and spectroscopy provide physiologic, quantifiable tumor data but can have threshold overlap and lack of technical standardization.[11]

DWI is widely integrated into clinical glioma MR imaging protocols with tissue properties measurable at the time of reporting. DWI exploits the inverse relationship between free water motion in tissues and cellularity.[12] Differences in diffusion-weighted image signals have been shown for glioma WHO grades and, more recently, between genetic subtypes.[13,14] The finding of lower ADC values in *IDH* wild-type diffuse glioma compared with *IDH* mutant tumors is consistently reported; however, the methods and accuracy vary among studies, whereby published techniques include mean and minimum ROI measurements and, in some cases, volumetric ADC quantification.[13-16] Hypothetically, "entire lesion" analysis might provide the most representative information on any individual tumor, whereas ROI placements have the advantage of being minimally time-consuming in clinical workflow.

There are few data comparing regional and volumetric diffusivity measurements for glioma genotyping, currently limited to nonenhancing glioma evaluation. The purpose of this study was to compare the performance of whole-tumor ADC measurements with different ROI parameters for glioma molecular typing, with a focus on *IDH* status prediction.

MATERIALS AND METHODS

Patients
Ethics review board approval (University College London Hospitals and Health Research Authority, United Kingdom) was obtained with informed consent waived for this retrospective imaging data study. Consecutive patients diagnosed at our national brain tumor referral institution from July 2008 to January 2018 were eligible for the research.

Inclusion criteria consisted of histologic confirmation of WHO grade II and III glioma, documented *IDH* and 1p19q genetic test results, and available pretreatment MR imaging. Exclusion criteria were previous glioma treatment; a diagnosis other than WHO grade II and III gliomas; incomplete, inconclusive, or ambiguous molecular results (eg, *IDH* wild-type/1p19q[codel]); a

prolonged (≥ year) interval from MR imaging to surgery; incomplete images; and failed volumetric image registration.

All tissue samples were analyzed at our neuropathology department, using the latest methodology according to the WHO 2016 Classification of CNS Tumors, as described previously.[17,18] Multiple gene Sanger sequencing was completed for *IDH* R132H-negative tumors to identify rarer *IDH* mutations, and the 1p/19q status was established through quantitative polymerase chain reaction–based copy number assay.

### MR Imaging Acquisition and Postprocessing
All MR imaging examinations included T2-weighted, T2-FLAIR, and T1-weighted sequences; pre- and postadministration of a gadolinium-based contrast agent; and DWI sequences (*n* = 211 at 1.5T, *n* = 79 at 3T). Because our institution is a quaternary center, the imaging originated from 23 different MR imaging machines with no individual scanner contributing >14% of any glioma subtype. In the generation of an ADC map, the image acquired without diffusion gradients is divided by the image acquired with diffusion gradients, removing dependence on T1, T2, and TR.[19] Sufficient comparability of ADC among scanners has been demonstrated previously.[20] The range of MR imaging parameters used has been described in a prior component of the study.[21] ADC maps were calculated from 3-directional DWI acquired with 2 gradient values ($b = 0$ and $b = 1000$ s/mm^2) using proprietary software (Olea Sphere, Version 2.3; Olea Medical).

ROI Measurements
The ADC regional measurements were performed by 3 independent observers as detailed in Maynard et al,[21] blinded to tissue diagnosis. First, each observer sited small (30–40 mm^2) ROIs 3× into the visually perceived lowest ADC portions of each glioma (within ≥1 axial image slice), while remaining in the solid tumor component and avoiding apparent necrotic, hemorrhagic, or cystic areas or blood vessels, as identified on the relevant accompanying contrast-enhanced and other sequences. From these 3 ROIs, the mean value of the numerically lowest ADC measurement was designated minimum ADC (ADC$_{min}$) as described in Xing et al.[14]

Thereafter, 1 large ROI (ADC$_{mean}$) was placed to cover most of the largest axial tumor cross-section, excluding tumor margins, necrosis, macroscopic hemorrhage, and calcifications, as described in Thust et al.[22] Finally, a comparative ROI was positioned in the contralateral normal-appearing centrum semiovale white matter (ADC$_{NAWM}$), amounting to 5 ROI measurements per patient. Multifocal tumors were measured as 1 glioma.

Observer 1 analyzed all (*n* = 290) gliomas, observer 2 re-analyzed a subset of 75 gliomas, and observer 3 re-analyzed the remaining subset of 215 gliomas, totaling 2900 ADC measurements (ie, 5 ROIs by 2 observers per glioma, ie, 10 × 290 measurements). From these, the normalized minimum ADC (rADC$_{min}$, defined as ADC$_{min}$/ADC$_{NAWM}$ ratio) and the mean normalized ADC (rADC$_{mean}$) (defined as ADC$_{mean}$/ADC$_{NAWM}$ ratio) were calculated, resulting in 4 regional ADC parameters (ROI ADC$_{min}$, ROI rADC$_{min}$, ROI ADC$_{mean}$, and ROI
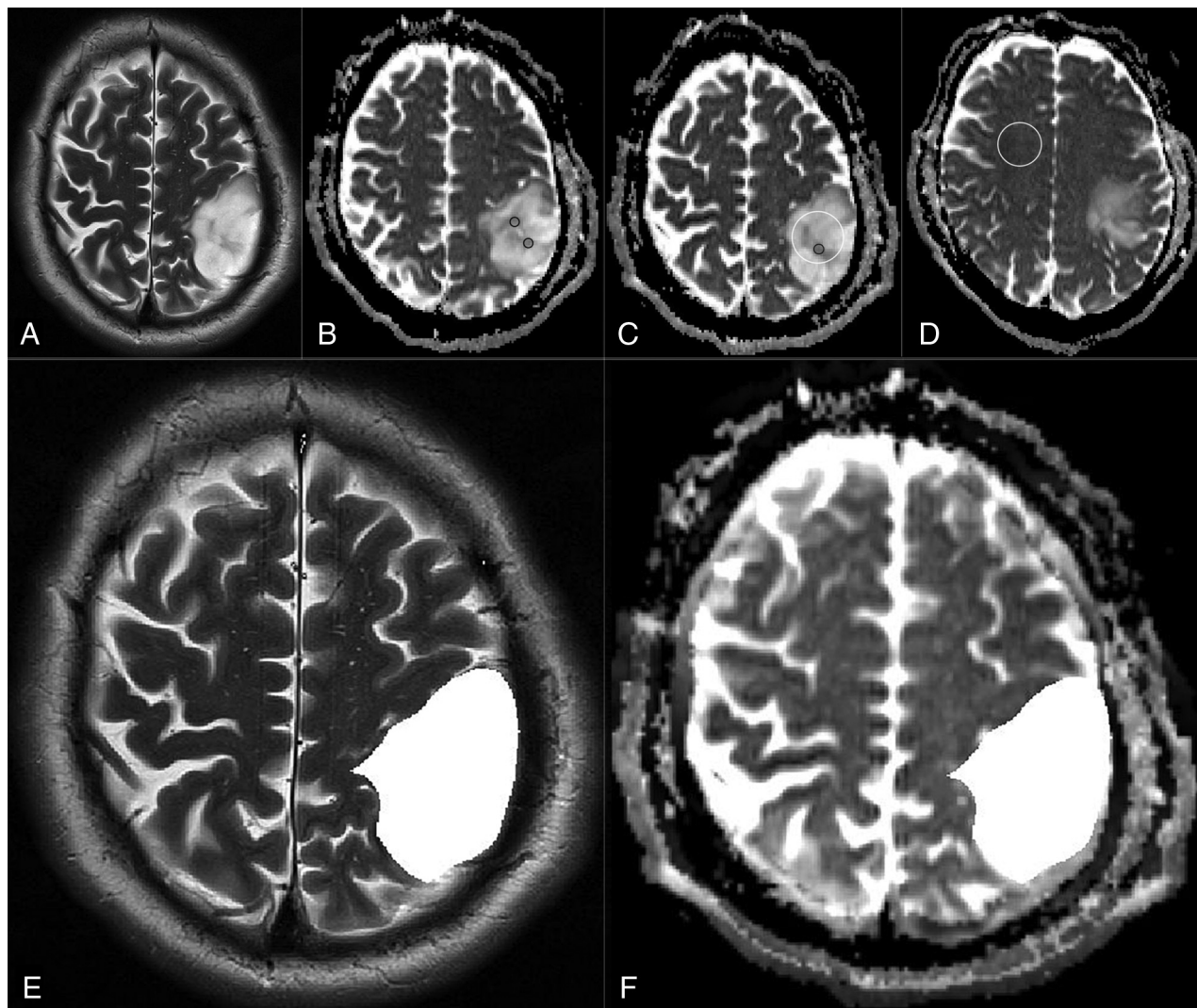
FIG 1. An example of regional and volumetric ADC measurements in a patient with *IDH* mutant 1p19q intact glioma. T2-weighted image (*A*) and ADC maps (*B–D*) show ADC_{min} (3 × 30–40 mm^2 (black, *B* and *C*), ADC_{mean} (white, *C*), and ADC_{NAWM} (white, *D*) ROI measurements. T2-weighted image (*E*) and ADC map (*F*) in the same patient demonstrate the volumetric segmentation and image registration, respectively.

$rADC_{mean}$) per glioma. An example of the ROI placements is shown in Fig 1*A–D*.

Volumetric ADC Histogram Analysis

Whole-tumor VOIs were segmented by a general radiologist (M.B., 5 years' experience) using the ITK-Snap Toolbox, Version 3.6 (www.itksnap.org[23]) following training and under supervision of a neuroradiologist specialized in brain tumor imaging (S.C.T, 9 years' experience). Segmentations incorporated the entire T2-weighted signal abnormality. For multicentric gliomas, the total volume of signal abnormality was treated as 1 lesion. To assess interobserver reproducibility, a proportion (10%) of gliomas was randomly chosen to undergo a repeat unsupervised segmentation by a second neuroradiologist (J.A.M., 4 years' experience, including brain tumor research).

ADC maps were then co-registered to T2-weighted sequences using the FMRIB Linear Image Registration Tool (FLIRT; http://www.fmrib.ox.ac.uk/fsl/fslwiki/FLIRT),[24,25] according to an affine 12-parameter model with the correlation ratio as a cost function, except in 15 cases in which manual review favored optimization of the registration by substitution of Normalized Mutual Information as the cost function. Subsequently, ADC histogram data were obtained for each tumor ROI, using an in-house script written in Python 2.7. For each tumor, the second and fifth ADC histogram percentiles, ADC mean, and the T2-weighted total lesion volume were extracted. Normalized histogram parameters were calculated using the same ROI ADC_{NAWM} value for the regional measurements to maximize direct comparability. An example of the volumetric segmentation is provided in Fig 1*E, -F*.

Enhancement Pattern Subgroup Analysis

Information on tumor enhancement, recorded as part of a preceding study,[21] was used for a subgroup analysis. Thus, the ability of ROI and VOI parameters to predict the *IDH* genotype was assessed separately for 3 morphologic groups: 1) nonenhancing, 2) solid-patchy enhancing, and 3) rim-enhancing, centrally necrotic gliomas. An example of the enhancement pattern distinction is provided in the Online Supplemental Data.

Patient demographics, *IDH*, and 1p19q genotypes of the study population

	All Glioma Subtypes	*IDH* Wild-Type	*IDH* Mutant/ 1p19q Intact	*IDH* Mutant/ 1p19q^{codel}
No. of patients = 283 (male/female = 164:119)	283	79	104	100
Median age (interquartile range) (yr)	40 (33–53)	59 (43–67)	35 (29–41)	40 (35–48)
Enhancement category[a]				
Nonenhancing	171	33	75	63
Solid-patchy enhancing	87	28	27	32
Rim-enhancing	23	18	0	5

Note:—1p19q^{codel} indicates codeletion of the short arm of chromosome 1 and the long arm of chromosome 19.
[a] In 2/283 patients, T1-weighted contrast-enhanced MR images were unavailable.

Statistical Analysis

All statistical testing was performed in SPSS 25 (IBM). The inter-observer agreement for the ROI-derived ADC measurements and for the volumetric segmentations was assessed by intraclass correlation coefficient analysis, using a 2-way random effects model. For each ADC ROI, the mean of the observers' measurements was adopted as the final value. For the proportion of tumors that were segmented by 2 observers, the average of the volumetric ADC results was designated as the final value.

To compare the mean ranks of the groups of ADC values and glioma subtypes, we used the nonparametric Kruskal-Wallis ANOVA test, including the Dunn pair-wise comparisons with Bonferroni correction. The strength of the association between glioma subtype and ADC metrics was tested using eta^2 (η^2), which quantifies the percentage of variance in the dependent variable (ADC value) that is explained by >1 independent variable (glioma genotype).

Univariable logistic regression was applied to test which ROI or VOI ADC parameter best predicted glioma *IDH* status (with $P < .05$ considered significant). The Youden index was used to identify diagnostic thresholds for the most predictive parameter, as determined by the area under the curve (AUC). Nonparametric (Wilcoxon signed rank) testing was performed to assess differences between the region-derived and volumetric ADC values.

RESULTS

Patient Demographics

Of 515 patients identified as potentially eligible for the study, 42 were duplicates, and 190 met the exclusion criteria as follows: previous glioma treatment ($n = 60$), tumor other than WHO grade II or III glioma ($n = 43$ and $n = 1$ spinal cord tumor), ambiguous or incomplete molecular results ($n = 29$), no preoperative DWI ($n = 24$ and $n = 15$ ADC maps not computable), unavailable histopathology report ($n = 2$), prolonged (≥ 1 year) interval from MR imaging to surgery ($n = 3$), MRI artefact ($n = 5$), incomplete images ($n = 1$), and failed volumetric image registration ($n = 7$). Finally, 283 patients (median, 40 years of age; interquartile range, 33–53 years; 164 men) were included in the analysis. The demographic details for the study population are listed in the Table.

Observer Comparison

The reproducibility of the ROI ADC parameters and contrast-enhancement patterns among 3 independent raters has been established in preceding research (intraclass correlation coefficient = 0.83–0.96 and Cohen κ = 0.69–0.72, respectively).[21] In the current study, the concordance between the 2 observers for the twice-segmented tumor volumes ($n = 28$) was near-complete (intraclass correlation coefficient = 0.97–0.98). This information is further detailed in the Online Supplemental Data.

Association between ADC Values and *IDH* Genotype

Box and whisker plots showing a comparison between *IDH* mutant and *IDH* wild-type gliomas for ADC$_{mean}$, rADC$_{mean}$, ADC$_{min}$, and rADC$_{min}$ are shown in the Online Supplemental Data (VOI and ROI methods). Detailed results from the statistical analysis with Kruskal-Wallis and η^2 tests are provided in the Online Supplemental Data. For all regional parameters (ROI ADC$_{min}$, ROI rADC$_{min}$, ROI ADC$_{mean}$, and ROI rADC$_{mean}$), the ADC values significantly differed among the *IDH* wild-type, *IDH* mutant, 1p19q intact, and *IDH* mutant 1p19q^{codel} glioma groups ($P < .001$). VOI ADC$_{mean}$ and VOI rADC$_{mean}$ also differed among the glioma molecular groups ($P < .001$).

VOI ADC$_{min}$ and VOI rADC$_{min}$ differed between *IDH* wild-type and *IDH* mutant 1p19q^{codel} genotypes ($P = .003$ and $P < .001$, respectively). However, no significant difference in VOI ADC$_{min}$ or VOI rADC$_{min}$ was shown between *IDH* mutant 1p19q intact and *IDH* mutant 1p19q^{codel} gliomas.

Wilcoxon signed rank testing confirmed statistically significant differences between the VOI and ROI results of the absolute and normalized ADC values ($P < .001$). The association between glioma genotype and diffusivity was strongest for ROI ADC$_{mean}$ and ROI rADC$_{mean}$ values ($\eta^2 = 0.38$) across the study population, while also being substantial for ROI ADC$_{min}$ and ROI rADC$_{min}$ ($\eta^2 = 0.28–0.29$).

The subgroup analysis according to the contrast-enhancement pattern revealed associations between ROI ADC$_{mean}$ and ROI rADC$_{mean}$ values and genotype for nonenhancing gliomas ($n = 170$, $\eta^2 = 0.39–0.41$) and solid-patchy enhancing gliomas ($n = 85$, $\eta^2 = 0.24–0.28$). No association was evident between ROI ADC parameters and the rim-enhancing, centrally necrotic glioma *IDH* genotype ($n = 23$, $\eta^2 = 0.0–0.05$). The strongest association for the rim-enhancing gliomas was with VOI rADC$_{mean}$ values ($\eta^2 = 0.36$).

No correlation among *IDH* status, VOI ADC$_{min}$, and VOI rADC$_{min}$ was identified for nonenhancing gliomas ($\eta^2 = 0.02–0.03$). Across all regional and volumetric parameters, smaller η^2 effect sizes were observed for minimum ADC values compared with mean ADC values. The VOI ADC$_{min}$ was tested as determined by either the 2nd or 5th percentile by histogram analysis, with consistently larger η^2 values observed between ADC$_{min}$ and genotype when the 5th percentile was used. Thereafter, VOI ADC$_{min}$ referred to the 5th percentile only.

ROC Curves for the prediction of *IDH* genotype in the study population (*n* = 283)
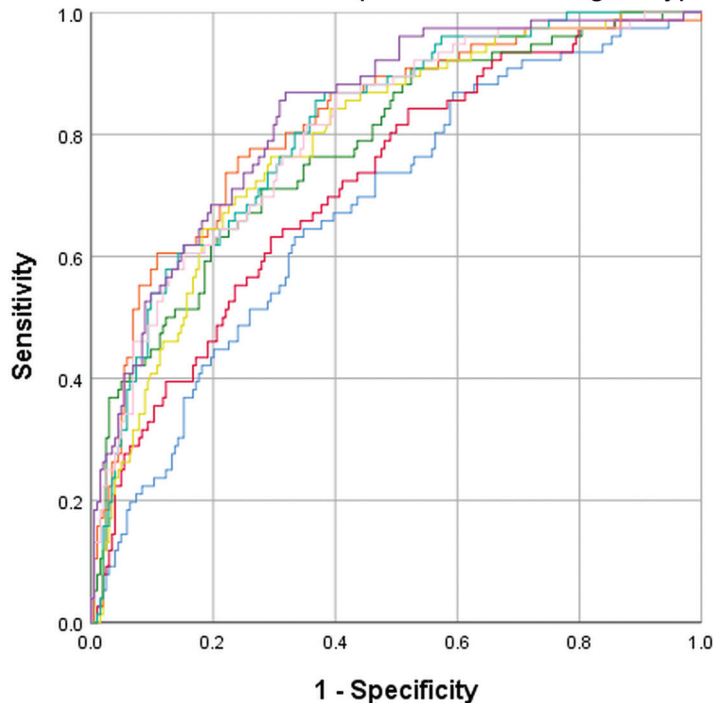
Area Under the ROC Curve (AUC)		
ADC metrics	Area Under the Curve	95% CI
VOI ADC$_{min}$	0.68	0.61 - 0.75
VOI rADC$_{min}$	0.72	0.66 - 0.79
VOI ADC$_{mean}$	0.78	0.72 - 0.84
VOI rADC$_{mean}$	0.82	0.76 - 0.88
ROI ADC$_{min}$	0.79	0.73 - 0.85
ROI rADC$_{min}$	0.81	0.76 - 0.86
ROI ADC$_{mean}$	0.81	0.75 - 0.86
ROI rADC$_{mean}$	0.83	0.78 - 0.89

FIG 2. ROC curves for the prediction of *IDH* genotype in the study population (*n* = 283).

Univariable Analysis for Prediction of IDH Status

The univariable analysis of regional and volumetric ADC metrics, when compared across all (*n* = 283) gliomas, showed that the most accurate prediction of *IDH* status was achieved using ROI rADC$_{mean}$ or VOI rADC$_{mean}$ (AUC = 0.83 and 0.82, respectively). The least accurate predictions were observed for VOI ADC$_{min}$ (AUC = 0.68) and VOI rADC$_{min}$ (AUC = 0.72). The ROC curve analysis is presented in Fig 2, with additional results listed in the Online Supplemental Data.

When assessing nonenhancing gliomas alone, the ROI ADC$_{mean}$ (AUC = 0.82) and ROI rADC$_{mean}$ (AUC = 0.84) results were almost equal to the VOI ADC$_{mean}$ (AUC = 0.81) and VOI rADC$_{mean}$ (AUC = 0.84). For solid-patchy tumors, the ROI ADC$_{mean}$ (AUC = 0.79) and ROI rADC$_{mean}$ (AUC = 0.81) were almost equal to the VOI ADC$_{mean}$ (AUC = 0.78) and VOI rADC$_{mean}$ (AUC = 0.80), respectively.

Conversely, in rim-enhancing centrally necrotic lesions, only volumetric ADC results demonstrated a significant ability to predict *IDH* status (VOI ADC$_{mean}$ [AUC = 0.84], VOI rADC$_{mean}$ [AUC = 0.90]), but not the ROI ADC$_{mean}$ and ROI rADC$_{mean}$ values (AUC = 0.49–0.61). Given the lack of an association between the volumetric ADC$_{min}$ parameters and *IDH* status, these were not further subjected to a subgroup analysis according to enhancement patterns.

DISCUSSION

This study investigated the comparability of region-derived and volumetric ADC values for WHO grade II and III glioma genotyping, specifically their performance for predicting *IDH* status. Our results indicate that the accuracy of regional measurements

for solid glioma *IDH* typing is unimproved by performing whole-tumor segmentations (maximum AUC = 0.84 for VOI and ROI rADC$_{mean}$). However, for *IDH* status prediction in the small proportion of rim-enhancing, centrally necrotic tumors (*n* = 23), entire lesion ADC mean parameters were superior to solid-tumor ROI measurements. Throughout the study, mean ADC measurements appeared more accurate than ADC$_{min}$ metrics, particularly if performing a volumetric analysis.

Before the discovery of glioma molecular subgroups, research was focused on testing the ability of ADC to predict glioma histologic grades, showing an inverse correlation between cellularity and diffusion.[26-28] More recently, Leu et al[13] demonstrated a stronger association between glioma ADC values and genotype than WHO grade. Specifically for *IDH* wild-type glioblastoma, no difference in diffusivity may exist between grades II and IV.[29] Villaneuva-Meyer et al[30] previously assessed ROI-derived minimum, mean, and maximum in WHO grade II gliomas: A minimum ADC threshold of 0.9×10^{-3} seconds/mm^2 provided the greatest sensitivity (91%) and specificity (76%) for *IDH* typing, with an AUC of 0.901.[19] ROI-based minimum ADC analysis was also performed by Wasserman et al[15] with a proposed cutoff point of 0.95×10^{-3} seconds/mm^2 (sensitivity of 76.9%, specificity of 65.2%, and AUC = 0.711)[13] and by Xing et al[14] with a suggested minimum ADC threshold of 1.01×10^{-3} seconds/mm^2 (sensitivity of 76.9%, specificity of 82.6%, AUC = 0.87).[15]

By means of ROI measurements, ADC$_{min}$ and rADC$_{min}$ appeared valuable for *IDH* typing in our study, with optimal thresholds in the region of 1.07×10^{-3} seconds/mm^2 (sensitivity of 82.3%, specificity of 61.3%, AUC = 0.79) and 1.40 (sensitivity of 85.5%, specificity of 62.3%, AUC = 0.81), respectively. For an ROI ADC$_{mean}$ threshold of 1.34×10^{-3} seconds/mm^2, a similar

sensitivity of 84.8%, specificity of 60.3%, and AUC of 0.81 were observed. For an $rADC_{mean}$ threshold of 1.75, the results were marginally better (sensitivity of 86.8%, specificity of 62.3, AUC = 0.83).

Across the whole study population, the largest ROI AUC (0.83) was observed for $rADC_{mean}$ values in our research. Liu et al[16] previously assessed glioma mean and minimum ADC, but only the results for mean ADC reached statistical significance ($P = .028$). Recently, in a study of normalized mean measurements for *IDH* typing of non-gadolinium-enhancing WHO grades II and III gliomas, an $rADC_{mean}$ threshold in the region of 1.8 was proposed.[22]

Several studies reported lower ADC values in *IDH* mutant 1p19q^{codel} oligodendrogliomas compared with *IDH* mutant 1p19q intact astrocytomas, with 2 studies indicating an ADC_{mean} threshold in the region of $1.4–1.6 \times 10^{-3 \text{ seconds}}/mm^2$ for 1p19q genotyping.[31,32] However, similar to the reduced specificity of elevated perfusion (blood volume), which may be observed in low-grade oligodendrogliomas, erroneously low ADC values can occur in this tumor type despite its relatively good prognosis. A potential influence from extracellular matrix components is probable.[33] It is also noteworthy that measurements in calcified tumor components may underestimate ADC values and should be avoided.

From our results, it appears that ROI ADC_{mean} and $rADC_{mean}$ are slightly superior to minimum ROI ADC measurements for *IDH* genotyping of WHO grade II and III gliomas. Similarly, Han et al[34] investigated the variability of ADC values according to the ROI technique for glioma grading, with the mean ADC value of single-round ROI showing the highest effect size (0.72) and the greatest AUC (0.872), being superior to minimum measurements for the identification of high-grade gliomas. Within the aforementioned study, minimum ADC values also differed significantly between whole-volume and single-round ROI placements ($P = .003$),[34] indicating that these are not interchangeable.

It has been shown that volumetric tumor diffusivity analysis is not necessarily superior to ROI placements, for example, for WHO grading.[35] In 2 recent studies using ADC for H3 K27M histone-mutant glioma characterization, only the study using ROI measurements was predictive of genotype.[36,37]

It could be hypothesized that the previously reported lower accuracy of ADC for WHO grade IV glioblastoma *IDH* typing[38] could be related to the foci of necrosis. However, in our current study, the best prediction of *IDH* status for such masses was achieved using VOI $rADC_{mean}$ values derived from segmentation inclusive of necrosis, as opposed to ROI measurement in solid lesion components. Indeed, our data suggest that partially necrotic tumors may benefit from a volumetric diffusivity (VOI $rADC_{mean}$) assessment, but the small patient number ($n = 23$) in this subgroup is a limitation of our research. Furthermore, it is possible that in some cases of necrotic tumors, limited tissue sampling resulted in a WHO grade II and III diagnosis instead of glioblastoma.

Imperfections in the volumetric image registration at glioma margins due to ADC map distortion from susceptibility gradients and eddy current effects, which are not visible in the T2-weighted image data, could have contributed to volumetric minimum ADC measurements performing less well in our research.

While the binary discrimination of *IDH* wild-type from *IDH* mutant gliomas is imperfect, noninvasive identification of early glioblastoma stages could help prioritize tissue sampling in such circumstances in which observational management is initially favored or when waiting times to surgery could result in a diagnostic delay.

CONCLUSIONS

Regional diffusivity measurements are noninferior and are possibly preferable to volumetric histogram analysis for *IDH* status prediction of macroscopically solid WHO grade II and III gliomas. ROI $rADC_{mean}$ calculation is rapid and scanner-independent, thus easily introduced into clinical reporting. Partially necrotic, rim-enhancing lesions are unsuitable for ROI assessment and may benefit from volumetric ADC quantification for genotyping.

REFERENCES

1. Brat DJ, Verhaak RG, Aldape KD, et al; Cancer Genome Atlas Research Network. **Comprehensive, integrative genomic analysis of diffuse lower-grade gliomas.** *N Engl J Med* 2015;372:2481–98 CrossRef Medline

2. Louis DN, Perry A, Reifenberger G, et al. **The 2016 World Health Organization Classification of Tumors of the Central Nervous System: a summary.** *Acta Neuropathol* 2016;131:803–20 CrossRef Medline

3. Stichel D, Ebrahimi A, Reuss D, et al. **Distribution of EGFR amplification, combined chromosome 7 gain and chromosome 10 loss, and TERT promoter mutation in brain tumors and their potential for the reclassification of *IDH* wild type astrocytoma to glioblastoma.** *Acta Neuropathol* 2018;136:793–803 CrossRef Medline

4. Tesileanu CM, Dirven L, Wijnenga MM, et al. Survival of diffuse astrocytic glioma, IDH1/2-wild type, with molecular features of glioblastoma, WHO grade IV: a confirmation of the cIMPACT-NOW criteria. *Neuro Oncol* 2020;22:515–23 CrossRef Medline

5. van den Bent MJ, Brandes AA, Taphoorn MJ, et al. **Adjuvant procarbazine, lomustine, and vincristine chemotherapy in newly diagnosed anaplastic oligodendroglioma: long-term follow-up of EORTC brain tumor group study 26951.** *J Clin Oncol* 2013;31:344–50 CrossRef Medline

6. Wijnenga MM, French PJ, Dubbink HJ, et al. **The impact of surgery in molecularly defined low-grade glioma: an integrated clinical, radiological, and molecular analysis.** *Neuro Oncol* 2018;20:103–12 CrossRef Medline

7. Kreth FW, Thon N, Simon M, et al. **Gross total but not incomplete resection of glioblastoma prolongs survival in the era of radiochemotherapy.** *Ann Oncol* 2013;24:3117–23 CrossRef Medline

8. Li YM, Suki D, Hess K, et al. **The influence of maximum safe resection of glioblastoma on survival in 1229 patients: can we do better than gross-total resection?** *J Neurosurg* 2016;124:977–88 CrossRef Medline

9. Mazurowski MA, Desjardins A, Malof JM. **Imaging descriptors improve the predictive power of survival models for glioblastoma patients.** *Neuro Oncol* 2013;15:1389–94 CrossRef Medline

10. Hyare H, Rice L, Thust S, et al. **Modelling MR and clinical features in grade II/III astrocytomas to predict *IDH* mutation status.** *Eur J Radiol* 2019;114:120–27 CrossRef Medline

11. Thust SC, Heiland S, Falini A, et al. **Glioma imaging in Europe: a survey of 220 centres and recommendations for best clinical practice.** *Eur Radiol* 2018;28:3306–17 CrossRef Medline

12. Patterson DM, Padhani AR, Collins DJ. **Technology insight: water diffusion MRI–a potential new biomarker of response to cancer therapy.** *Nat Clin Pract Oncol* 2008;5:220–33 CrossRef Medline

13. Leu K, Ott GA, Lai A, et al. **Perfusion and diffusion MRI signatures in histologic and genetic subtypes of WHO grade II-III diffuse gliomas.** *J Neurooncol* 2017;134:177–88 CrossRef Medline

14. Xing Z, Yang X, She D, et al. **Noninvasive assessment of *IDH* mutational status in World Health Organization grade II and III astrocytomas using DWI and DSC-PWI combined with conventional MR imaging.** *AJNR Am J Neuroradiol* 2017;38:1138–44 CrossRef Medline

15. Wasserman JK, Nicholas G, Yaworski R, et al. **Radiological and pathological features associated with IDH1-R132H mutation status and early mortality in newly diagnosed anaplastic astrocytic tumours.** *PLoS One* 2015;10:e0123890 CrossRef Medline

16. Liu T, Cheng G, Kang X, et al. **Noninvasively evaluating the grading and IDH1 mutation status of diffuse gliomas by three-dimensional pseudo-continuous arterial spin labeling and diffusion-weighted imaging.** *Neuroradiology* 2018;60:693–702 CrossRef Medline

17. Jaunmuktane Z, Capper D, Jones DTW, et al. **Methylation array profiling of adult brain tumours: diagnostic outcomes in a large, single centre.** *Acta Neuropathol Commun* 2019;7:24 CrossRef Medline

18. Reuss DE, Sahm F, Schrimpf D, et al. **ATRX and IDH1-R132H immunohistochemistry with subsequent copy number analysis and *IDH* sequencing as a basis for an "integrated" diagnostic approach for adult astrocytoma, oligodendroglioma and glioblastoma.** *Acta Neuropathol* 2015;129:133–46 CrossRef Medline

19. Pipe J. Pulse sequences for diffusion-weighted MRI. In: Johansen-Berg H, Behrens TE, eds. *Diffusion MRI*. Academic Press; 2009;11–35

20. Grech-Sollars M, Hales PW, Miyazaki K, et al. **Multi-centre reproducibility of diffusion MRI parameters for clinical sequences in the brain.** *NMR Biomed* 2015;28:468–85 CrossRef Medline

21. Maynard J, Okuchi S, Wastling S, et al. **World Health Organization grade II/III glioma molecular status: prediction by MRI morphologic features and apparent diffusion coefficient.** *Radiology* 2020;296:111–21 CrossRef Medline

22. Thust SC, Hassanein S, Bisdas S, et al. **Apparent diffusion coefficient for molecular subtyping of non-gadolinium-enhancing WHO grade II/III glioma: volumetric segmentation versus two-dimensional region of interest analysis.** *Eur Radiol* 2018;28:3779–88 CrossRef Medline

23. Yushkevich PA, Piven J, Hazlett HC, et al. **User-guided 3D active contour segmentation of anatomical structures: significantly improved efficiency and reliability.** *Neuroimage* 2006;31:1116–28 CrossRef Medline

24. Jenkinson M, Bannister P, Brady M, et al. **Improved optimization for the robust and accurate linear registration and motion correction of brain images.** *Neuroimage* 2002;17:825–41 CrossRef Medline

25. Jenkinson M, Smith S. **A global optimisation method for robust affine registration of brain images.** *Med Image Anal* 2001;5:143–56 CrossRef Medline

26. Louis DN, Ohgaki H, Wiestler OD, et al. **The 2007 WHO Classification of Tumours of the Central Nervous System.** *Acta Neuropathol* 2007;114:97–109 CrossRef Medline

27. Hilario A, Ramos A, Perez-Nuñez A, et al. **The added value of apparent diffusion coefficient to cerebral blood volume in the preoperative grading of diffuse gliomas.** *AJNR Am J Neuroradiol* 2012;33:701–07 CrossRef Medline

28. Sugahara T, Korogi Y, Kochi M, et al. **Usefulness of diffusion-weighted MRI with echo-planar technique in the evaluation of cellularity in gliomas.** *J Magn Reson Imaging* 1999;9:53–60 CrossRef Medline

29. Figini M, Riva M, Graham M, et al. **Prediction of isocitrate dehydrogenase genotype in brain gliomas with MRI: single-shell versus multishell diffusion models.** *Radiology* 2018;289:788–96 CrossRef Medline

30. Villanueva-Meyer JE, Wood MD, Choi BS, et al. **MRI Features and *IDH* Mutational Status of Grade II Diffuse Gliomas: Impact on Diagnosis and Prognosis.** *American Journal of Roentgenology* 2018;210:621–28 CrossRef Medline

31. Johnson DR, Diehn FE, Giannini C, et al. **Genetically defined oligodendroglioma is characterized by indistinct tumor borders at MRI.** *AJNR Am J Neuroradiol* 2017;38:678–84 CrossRef Medline

32. Cui Y, Ma L, Chen X, et al. **Lower apparent diffusion coefficients indicate distinct prognosis in low-grade and high-grade glioma.** *J Neurooncol* 2014;119:377–85 CrossRef Medline

33. Sadeghi N, Camby I, Goldman S, et al. **Effect of hydrophilic components of the extracellular matrix on quantifiable diffusion-weighted imaging of human gliomas: preliminary results of correlating apparent diffusion coefficient values and hyaluronan expression level.** *AJR Am J Roentgenol* 2003;181:235–41 CrossRef Medline

34. Han X, Suo S, Sun Y, et al. **Apparent diffusion coefficient measurement in glioma: Influence of region-of-interest determination methods on apparent diffusion coefficient values, interobserver variability, time efficiency, and diagnostic ability.** *J Magn Reson Imaging* 2017;45:722–30 CrossRef Medline

35. Takano K, Kinoshita M, Arita H, et al. **Influence of region-of-interest designs on quantitative measurement of multimodal imaging of MR non-enhancing gliomas.** *Oncol Lett* 2018;15:7934–40 CrossRef Medline

36. Aboian MS, Tong E, Solomon DA, et al. **Diffusion characteristics of pediatric diffuse midline gliomas with histone H3-K27M mutation using apparent diffusion coefficient histogram analysis.** *AJNR Am J Neuroradiol* 2019;40:1804–10 CrossRef Medline

37. Chen H, Hu W, He H, et al. **Noninvasive assessment of H3 K27M mutational status in diffuse midline gliomas using apparent diffusion coefficient measurements.** *Eur J Radiol* 2019;114:152–59 CrossRef Medline

38. Tan WL, Huang WY, Yin B, et al. **Can diffusion tensor imaging noninvasively detect IDH1 gene mutations in astrogliomas? A retrospective study of 112 cases.** *AJNR Am J Neuroradiol* 2014;35:920–97 CrossRef Medline